

# Spin and density overlaps in the frustrated Ising lattice gas

Antonio de Candia and Antonio Coniglio

*Dipartimento di Scienze Fisiche*

*INFN, Unità di Napoli*

*Monte Sant'Angelo, I-80126 Napoli, Italy*

We perform large scale simulations of the frustrated Ising lattice gas, a three-dimensional lattice model of a structural glass, using the parallel tempering technique. We evaluate the spin and density overlap distributions, and the corresponding non-linear susceptibilities, as a function of the chemical potential. We then evaluate the relaxation functions of the spin and density self-overlap, and study the behavior of the relaxation times. The results suggest that the spin variables undergo a transition very similar to the one of the Ising spin glass, while the density variables do not show any sign of transition at the same chemical potential. It may be that the density variables undergo a transition at a higher chemical potential, inside the phase where the spins are frozen.

## I. INTRODUCTION

In the last years, a scenario has emerged for the theoretical description of structural glasses, in which the behavior of glasses is characterized by two different temperatures. The higher temperature  $T_c$ , identified with the critical temperature of the ideal mode-coupling theory [1], corresponds to a crossover in the dynamical behavior of the glass, characterized by a single relaxation time for  $T > T_c$ , and by a two-step relaxation for  $T < T_c$ . Below  $T_c$ , the free energy landscape in the phase space is splitted into an extensive number of valleys, separated by high barriers, and the dynamics is separated in a fast motion inside the valley, and a much slower motion among different valleys. The number of valleys accessible to the system at the temperature  $T$ , can be expressed by the formula  $\mathcal{N} = \exp(N\Sigma(T))$ , where  $N$  is the number of particles in the system, and  $\Sigma(T)$  is the so-called configurational entropy. The second temperature  $T_K$ , identified with the Kauzmann temperature [2] and the critical temperature of the Adam and Gibbs theory [3], is characterized by the vanishing of the configurational entropy  $\Sigma(T)$ , and the divergence of the relaxation time of the system with a Vogel-Fulcher-Tamman law.

This picture is corroborated by the analogy with a class of mean field models, the  $p$ -spin glasses. These models undergo a dynamical transition at a temperature  $T_d$ , where the phase space splits into an extensive number of metastable states, and the correlation functions show a singularity of the same type of the one predicted by mode-coupling theory [4]. At a lower temperature  $T_s$  the number of metastable states becomes non-extensive, that is the configurational entropy vanishes, and for  $T < T_s$  the model shows a 1-step replica symmetry breaking. It has been longly debated to what extent this analogy, between structural glasses and  $p$ -spin models, can be pushed forward. In particular one may ask if structural glasses exhibit some kind of replica symmetry breaking, and if they are in the same universality class of  $p$ -spin models or not. There are presently

some results that point in this direction. First principle computations of the equilibrium thermodynamics of simple fragile glasses seem to be consistent with this picture [5], and the off-equilibrium fluctuation-dissipation ratio, in molecular dynamics simulations of supercooled liquids [6], shows the same pattern observed in  $p$ -spin glasses and predicted for 1-step RSB models [7,8].

Nevertheless, there are still some important differences between structural glasses and  $p$ -spin models. In  $p$ -spin glasses the relevant variables are the spin orientations, and there is explicit quenched disorder in the Hamiltonian. On the other hand, in glasses the relevant variables are the particle positions, and there are no quenched interactions in the Hamiltonian, but the disorder is “self-generated” by the geometrical hindrance that the particles exert on each other. Furthermore,  $p$ -spin glasses are mean-field models, while structural glasses live in finite dimension. This means among other things that metastable states in  $p$ -spin models have infinite lifetime, and the dynamical transition  $T_d$  corresponds to a divergence of the relaxation times, while in finite dimensional models the barriers between free energy valleys can be overcome by “hopping” processes, which restore ergodicity even below the crossover temperature  $T_c$ . Furthermore the  $p$ -spin model, if studied in three dimensions, loses many of its mean field “glassy” properties, and shows a transition similar to the full replica symmetry breaking transition of Ising spin glasses, though with some remarkable differences [9].

The frustrated Ising lattice gas was introduced some time ago as a simple finite dimensional lattice model of a glass-forming liquid [10], in order to overcome some of the limitations of  $p$ -spin models. Each lattice site carries two kinds of variables, a lattice gas variable  $n_i = 0, 1$ , which represent the presence or absence of a particle on the  $i$ -th site, and an Ising spin variable  $S_i$ , which represent an internal degree of freedom of the particle, such as for example the orientation of a non-symmetrical molecule. The Hamiltonian of the model is

$$\mathcal{H} = J \sum_{\langle ij \rangle} (1 - \epsilon_{ij} S_i S_j) n_i n_j - \mu \sum_i n_i, \quad (1)$$

where  $\epsilon_{ij} = \pm 1$  are quenched variables. In the limit  $J \rightarrow \infty$ , the first term of the Hamiltonian implies that two nearest neighbor sites can be simultaneously occupied by two particles only if their spin variables satisfy the constraint  $\epsilon_{ij} S_i S_j = 1$ . Therefore, if we identify the variables  $S_i$  with the orientation of a non-symmetrical molecule, this condition means that two molecules can be near only if their relative orientation is appropriate.

Being constituted essentially by diffusing particles, this model is suited to study quantities like the diffusion coefficient, or the density autocorrelation functions, that are usually important in the study of liquids. Indeed, the model has proven to reproduce fairly well many features of supercooled glass-forming liquids, as for example the ‘‘cage effect’’. At low temperature and high density, the model shows a two step relaxation in the self correlation function and in the mean square displacement. Furthermore, being a finite dimensional model, it is suitable to study activated processes, that are absent in mean field models.

Although the model has been extensively studied by Monte Carlo simulations [10] and in mean field [11], there are still many unsolved problems, concerning the type of transition presented by the model. In particular, it would be interesting to study if, in finite dimension, density and spin variables become critical at the same point, and what kind of replica symmetry breaking they show in the spin glass phase.

In this paper, we study the static and dynamical equilibrium properties of the model in the limit  $J \rightarrow \infty$ . We will evaluate the equilibrium overlap distribution of spin and density variables, the equilibrium autocorrelation functions of the self-overlaps, and the self-diffusion coefficient.

## II. SPIN AND DENSITY OVERLAP DISTRIBUTIONS

We have simulated the frustrated Ising lattice gas by means of the parallel tempering technique [12,13]. With this technique one can thermalize the system at high chemical potential (high density), where the conventional Monte Carlo algorithms suffer of extremely long autocorrelation times. One has to simulate several identical replicas of the system, at different chemical potentials  $\mu_0 < \dots < \mu_n$ , where  $\mu_0$  corresponds to a low density and very short autocorrelation time, and  $\mu_n$  to the highest value of the chemical potential that one wants to investigate. Each step of the algorithm consists of the following two substeps: for each replica, perform a conventional Monte Carlo step with the given temperature and chemical potential; for each pair of replicas with adjacent chemical potentials, try to swap them with probability  $P_{\text{swap}} = \min(1, \exp(-\beta \Delta \mu \Delta n))$ , where  $\Delta n$  is the

difference in the number of particles of the two replicas considered, and  $\Delta \mu$  the difference of their chemical potentials. If one chooses carefully the set of chemical potentials, then the replicas will perform a random walk over the interval  $[\mu_0, \mu_n]$ . The time needed to go from  $\mu_0$  to  $\mu_n$  and back again is called *ergodic time*, and can be considered as the maximum autocorrelation time of the system.

We have simulated the model for  $J = \infty$  and  $\beta = 1$ , between the chemical potentials  $\mu_{\min} = 1.69$  and  $\mu_{\max} = 10.69$ , for system sizes  $6^3$ ,  $8^3$  and  $10^3$ . In the first case we have performed the simulation over 12 values of the chemical potential, in the second over 16 values, and in the third over 25 values. The exact values of the chemical potentials were determined by an algorithm which tried to optimize the intervals, in order to obtain the same swap rate between all the adjacent replicas. For each value of the chemical potential we simulated two replicas, in order to evaluate spin and density overlap. The thermalization of the systems was checked by looking at the densities of the replicas, and waiting until they did not show any sensible drift in time. The thermalization time was greater than  $10^6$  steps.

After having thermalized the systems, at each parallel tempering step we collected, for each pair of replicas at the same chemical potential, the spin overlap  $q_s = \frac{1}{N} \sum_i S_i^\alpha n_i^\alpha S_i^\beta n_i^\beta$  and the density overlap  $q_d = \frac{1}{N} \sum_i n_i^\alpha n_i^\beta$ , where the superscripts  $\alpha$  and  $\beta$  refer to the two replicas, and  $N$  is the number of spins. We simulated the systems for up to  $10^7$  steps for the largest size, and checked the symmetry of the spin overlap distribution to be sure that the simulation time was sufficient. All the relevant quantities were averaged over 32 disorder realizations, and errors were evaluated from the fluctuations between different realizations.

In Fig. 1 the equilibrium distribution of the spin overlap is shown, for the largest size  $10^3$  and for different chemical potentials. For high chemical potential, the distribution develops two peaks, separated by a continuous plateau. This is typical of models with a continuous replica symmetry breaking, like the Ising spin glass in three dimensions. Note that, for the highest chemical potential, the distribution between the two peaks is not a constant plateau, but is formed by many small peaks. This can be due to the fact that, at high chemical potential or low temperature, averaging over more than 32 disorder realizations is needed to obtain a constant plateau. The continuous replica symmetry breaking is associated with the divergence of the spin glass susceptibility, defined as  $\chi_{SG} = N \langle q_s^2 \rangle$ , where  $\langle \dots \rangle$  denotes both the thermal average for a given set of interactions and the average over the disorder realizations. We have evaluated  $\chi_{SG}$  for the different sizes and chemical potential, and the result is shown in Fig. 2. The behavior of the susceptibility confirms the presence of a thermodynamical second order transition. The exact value of the chemical potential at the transition can be evaluated by

looking at the Binder parameter  $g = \frac{1}{2}(3 - \langle q_s^4 \rangle / \langle q_s^2 \rangle^2)$ , that is shown in Fig. 3. The curves corresponding to the different sizes cross at the chemical potential  $\mu_c = 3.67$ . Once we have located the transition, we can try to evaluate the critical exponents, using the relation  $\chi_{SG}(L, \mu) = L^{2-\eta} \tilde{\chi}_{SG}[L^{1/\nu}(\mu - \mu_c)]$ , that should be valid around the transition, with  $\tilde{\chi}_{SG}[x]$  a universal curve. In Fig. 4 the best fit is shown, obtained for the values  $\eta = 0$  and  $\nu = 1$ . Note that these exponents were obtained also by Campellone *et al.* [9] in the three-dimensional version of the  $p$ -spin model. They are different from the exponents found in the Ising spin glass,  $\nu = 1.7 \pm 0.3$  and  $\eta = -0.35 \pm 0.05$  [14]. This suggests that the transition could belong to a different universality class with respect to the Ising spin glass.

We have then evaluated the equilibrium distribution of the density overlap, which is shown in Fig. 5 for the largest size and for different chemical potentials. The non-linear compressibility  $\kappa_{nl} = N(\langle q_d^2 \rangle - \langle q_d \rangle^2)$  is shown in Fig. 6 as a function of the chemical potential. The arrow in Fig. 6 marks the point where the spin variables undergo the transition, as signaled by the crossing of the Binder parameter, and the spin glass susceptibility diverges. It is evident that this point does not correspond to a divergence of the non-linear compressibility. Therefore the divergence of the spin glass susceptibility is due to the fluctuations of spin variables  $S_i$ , and not to the fluctuations of the density variables  $n_i$ . We have also evaluated the Binder parameter of the density overlap (not shown), which shows a non-monotonic behavior, becoming negative for low density and positive at high density, similarly to what is observed in the finite-dimensional  $p$ -spin [9]. Indeed the curves for different sizes do not cross at a definite point, so they cannot be used to localize the transition (if any) of the density variables.

It remains to be determined whether or not the density variables exhibit a transition not manifested by a divergence of the non-linear compressibility. Note that for very high chemical potential the equilibrium distribution of the density overlap develops a secondary minimum. This could correspond to a transition of different kind, perhaps similar to the 1-step replica symmetry breaking transition of the  $p$ -spin models.

### III. RELAXATION FUNCTIONS OF SPIN AND DENSITY SELF-OVERLAP

The frustrated Ising lattice gas is known to have very large relaxation times at high density or low temperature [10]. Here we want to evaluate the relaxation times of the spin self-overlap, defined as  $q_s(t) = \frac{1}{N} \sum_i \langle S_i(t') n_i(t') S_i(t'+t) n_i(t'+t) \rangle$ , and the density self-overlap  $q_d(t) = \frac{1}{N} \sum_i (\langle n_i(t') n_i(t'+t) \rangle - \langle n_i(t') \rangle^2)$ , where the average  $\langle \dots \rangle$  is done over the reference time  $t'$ . We have simulated the model for system size  $20^3$ , and 10

chemical potentials between  $\mu = 2.583$  and  $3.661$ , in the following manner. We start with an empty system, with the interactions randomly chosen, thermalize at the given chemical potential for a given time  $\Delta t$ , save the obtained configuration, and then simulate the model saving the self-overlaps  $q_s(t)$  and  $q_d(t)$  with respect to the configuration at the end of thermalization. Then we repeat the process again with a different disorder configuration and thermal noise. The thermalization time  $\Delta t$  is at least 10 times larger than the time needed to the self-overlap to decay to the value 0.1, except for the three highest chemical potentials, for which the thermalization time was shorter. The self-overlaps were averaged over at least 100 different runs, and errors were evaluated from the fluctuations between different runs. When evaluating the density self-overlap  $q_d(t)$ , the quantity  $\frac{1}{N} \sum_i \langle n_i(t') \rangle^2$  can be taken equal to the average density overlap  $\langle q_d \rangle$  at equilibrium, as calculated in the parallel tempering simulations.

In Fig. 7 the relaxation functions of the spin self-overlap are shown. The solid lines are fit with the function  $ct^{-x} \exp(-(t/\tau)^\beta)$ , proposed by Ogielski for the Ising spin glass [15]. The exponent  $\beta$  is nearly constant within the errors for all the chemical potentials considered, and slightly greater than 0.5, while the exponent  $x$  varies between 0.2 for the lowest chemical potential to 0.1 for the highest. The correlation times  $\tau$  are shown in Fig. 8, excluding the last three points, which are likely to suffer from insufficient thermalization or finite size effects. A power law fit  $\tau \sim |\mu - \mu_c|^{-z\nu}$  gives a dynamical exponent  $z = 7.4$ , slightly greater than the exponent  $z = 6.0 \pm 0.8$  found by Ogielski for the Ising spin glass.

In Fig. 9 the relaxation functions of the density self-overlap are shown, for the same system size and chemical potentials. Note that the relaxation times grow very slowly with respect to those of the spin self-overlap. This supports the conclusion that the transition at  $\mu_c = 3.67$  does not involve the density variables  $n_i$ . The latter probably undergo a transition at a higher chemical potential, inside the phase where the spin variables are frozen.

## IV. DIFFUSIVITY

We have simulated the model with a purely diffusive dynamics, in the following way. We start with an empty lattice, with random interactions, and then slowly raise the chemical potential, until a given density is reached. Then we switch to a purely diffusive dynamics, with conserved number of particles, and thermalize the system at the given density. After having thermalized the system, we collect the mean square displacement  $\langle r^2(t) \rangle$  of the particles as a function of time. The long time regime of the mean square displacement is of the form  $\langle r^2(t) \rangle = Dt$ , from which we extract the diffusion coefficient  $D$ . To each density, we associate a chemical potential from the equilibrium relation between the two quantities.

In Fig. 10 the diffusion coefficient  $D$  is shown for a system size  $16^3$  as a function of the chemical potential. For high chemical potential, it can be well fitted by an Arrhenius form,  $D = ae^{-\alpha\mu}$ . Therefore, the diffusion of the particles seems to stop only at  $\mu \rightarrow \infty$ , which corresponds to  $T \rightarrow 0$ . The arrow marks the point where the spin variables undergo the spin glass-like transition: apparently no anomaly in the diffusivity shows up in correspondence of the transition. In the inset, the diffusivity as a function of the density is shown. Note that for  $\mu \rightarrow \infty$  the density goes to a maximum value  $\rho_{\max} \simeq 0.68$ . The diffusivity can be well fitted by a power law  $D = a(\rho_0 - \rho)^\gamma$ , where  $\rho_0 = 0.681$  and  $\gamma = 1.38$ .

## V. CONCLUSIONS

We have studied the static and dynamical properties of the frustrated Ising lattice gas at equilibrium. A spin glass-like transition is found in the spin variables, signaled by the crossing of the Binder parameter, the divergence of the non-linear susceptibility, and the development of a continuous replica symmetry breaking in the spin overlap distribution. The equilibrium autocorrelation functions of the spin overlap can be well fitted by an Ogielsky form, with a correlation time diverging at the critical point. On the other hand, the density variables seem to be affected little by the transition, showing no divergence either in the non-linear compressibility, or in the autocorrelation time.

The freezing of the model at the chemical potential  $\mu_c$  is therefore connected with a second order transition in the spin variables, more similar to the freezing of the Ising spin glass than to the mode-coupling transition of structural glasses. One cannot exclude that the density variables undergo a  $p$ -spin-like transition at a higher density, characterized by a 1-step replica symmetry breaking and a discontinuity of the Edwards-Anderson parameter defined in terms of density variables. This fact is suggested by the development of a secondary peak in the density overlap distribution at very high chemical potential, as well as by the measurements of the off-equilibrium fluctuation-dissipation ratio [16], but more work is needed to clarify this point.

## ACKNOWLEDGMENTS

This work was partially supported by the European TMR Network-Fractals (Contract No. FMRXCT980-183), MURST-PRIN-2000 and INFMPRA(HOP). We acknowledge the allocation of computer resources from INFN Progetto Calcolo Parallelo.

- [1] W. Götze, in *Liquids, Freezing and the Glass Transition*, eds. J.P. Hansen, D. Levesque, J. Zinn-Justin, (North Holland 1990).
- [2] W. Kauzmann, *Chem. Rev.* **43**, 219 (1948).
- [3] G. Adam and J.H. Gibbs, *J. Chem. Phys.* **43**, 139 (1965).
- [4] T.R. Kirkpatrick and D. Thirumalai, *Phys. Rev. B* **36**, 5388 (1987); T.R. Kirkpatrick and P.G. Wolynes, *Phys. Rev. B* **36**, 8552 (1987).
- [5] R. Monasson, *Phys. Rev. Lett.* **75**, 2847 (1995); M. Mézard and G. Parisi, *Phys. Rev. Lett.* **82**, 747 (1998); M. Mézard and G. Parisi, *J. Chem. Phys.* **111**, 1076 (1999).
- [6] G. Parisi, *Phys. Rev. Lett.* **79**, 3660 (1997); G. Parisi, *Phil. Mag. B* **77**, 257 (1998); W. Kob and J.L. Barrat, *Europhys. Lett.* **46**, 637 (1999); F. Sciortino and P. Tartaglia, *Phys. Rev. Lett.* **86**, 107 (2001).
- [7] L.F. Cugliandolo and J. Kurchan, *Phys. Rev. Lett.* **71**, 173 (1993).
- [8] S. Franz, M. Mezard, G. Parisi, and L. Peliti, *Phys. Rev. Lett.* **81**, 1758 (1998).
- [9] M. Campellone, B. Coluzzi, G. Parisi, *Phys. Rev. B* **58**, 12081 (1998); M. Campellone, G. Parisi, P. Ranieri, *Phys. Rev. B* **59**, 1036 (1999).
- [10] M. Nicodemi and A. Coniglio, *J. Phys. A* **30**, L187 (1997); M. Nicodemi and A. Coniglio, *Phys. Rev. E* **57**, R39 (1998); A. Coniglio, A. de Candia, A. Fierro and M. Nicodemi, *J. Phys. Cond. Mat.* **11**, A167 (1999); A. Fierro, A. de Candia and A. Coniglio, *Phys. Rev. E* **62**, 7715 (2000); J.J. Arenzon, F. Ricci-Tersenghi, and D.A. Stariolo, *Phys. Rev. E* **62**, 5978 (2000).
- [11] S.K. Ghatak and D. Sherrington, *J. Phys. C* **10** 3149 (1977); F.A. da Costa, C.S.O. Yokoi and S.R.A. Salinas, *J. Phys. A* **27**, 3365 (1994); J.J. Arenzon, M. Nicodemi and M. Sellitto, *J. de Physique* **6**, 1143 (1996); M. Sellitto, M. Nicodemi and J.J. Arenzon, *J. de Physique* **7**, 945 (1997); H. Feldmann and R. Oppermann, *J. Phys. A* **33**, 1325 (2000).
- [12] K. Hukushima and K. Nemoto, *cond-mat/9512035*.
- [13] E. Marinari, G. Parisi and J.J. Ruiz-Lorenzo, in *Spin Glasses and Random Fields*, ed. A.P. Young (World Scientific, Singapore, 1997), *cond-mat/9701016*.
- [14] N. Kawashima and A.P. Young, *Phys. Rev. B* **53**, R484 (1996).
- [15] A.T. Ogielski, *Phys. Rev. B* **32**, 7384 (1985).
- [16] F. Ricci-Tersenghi, D.A. Stariolo, and J.J. Arenzon, *Phys. Rev. Lett.* **84**, 4473 (2000); A. de Candia and A. Coniglio, *Phys. Rev. Lett.* **86**, 4716 (2001); F. Ricci-Tersenghi, G. Parisi, D.A. Stariolo, and J.J. Arenzon, *Phys. Rev. Lett.* **86**, 4717 (2001).

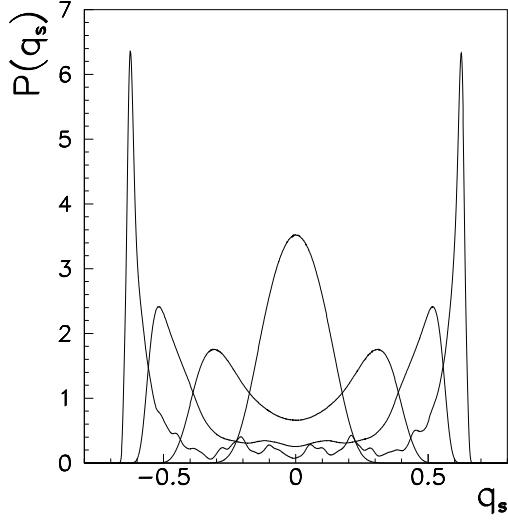


FIG. 1. Spin overlap distribution  $P(q_s)$  for size  $10^3$  and chemical potentials  $\mu=3.08, 4.12, 5.79, 10.69$ .

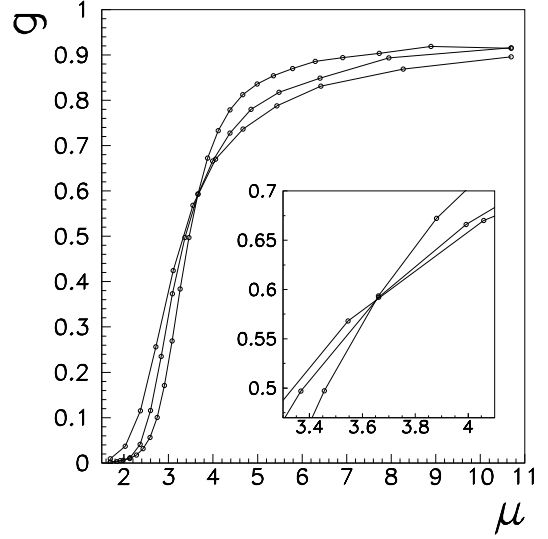


FIG. 3. Binder parameter  $g$  as a function of the chemical potential, for sizes  $6^3, 8^3$  and  $10^3$ . Inset: the point where the curves cross, at  $\mu = 3.67$ .

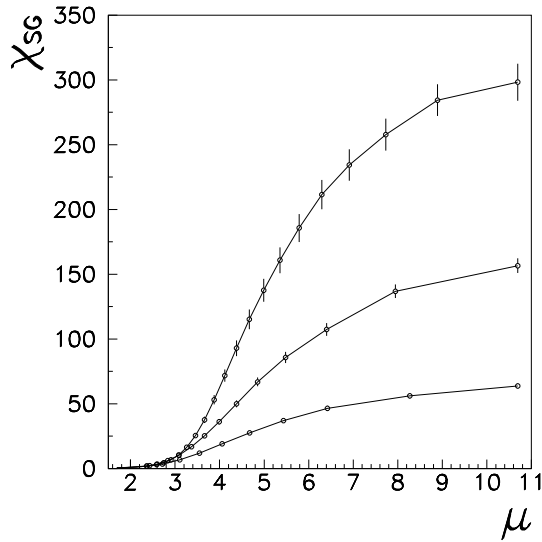


FIG. 2. Spin glass susceptibility  $\chi_{SG}$  as a function of the chemical potential, for sizes  $6^3, 8^3$  and  $10^3$ .

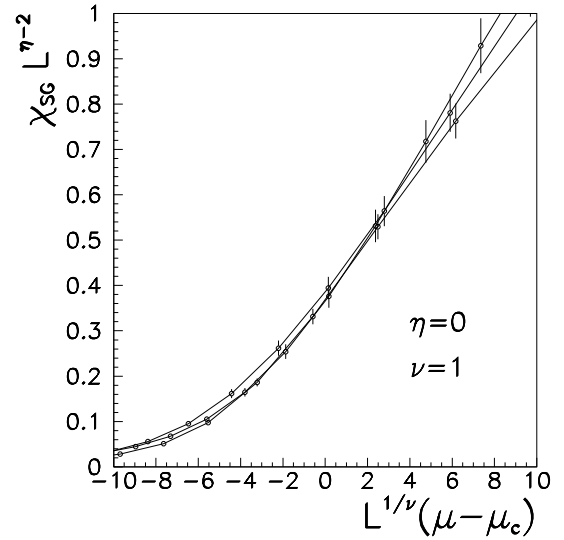


FIG. 4. Finite size scaling plot of the spin glass susceptibility, with  $\mu_c = 3.67$ . The exponents that give the best data collapse are  $\eta = 0$  and  $\nu = 1$ .

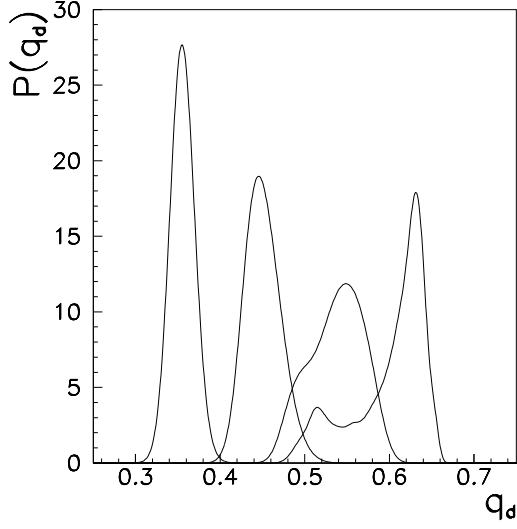


FIG. 5. Density overlap distribution  $P(q_d)$  for size  $10^3$  and chemical potentials  $\mu=3.08, 4.12, 5.79, 10.69$ .

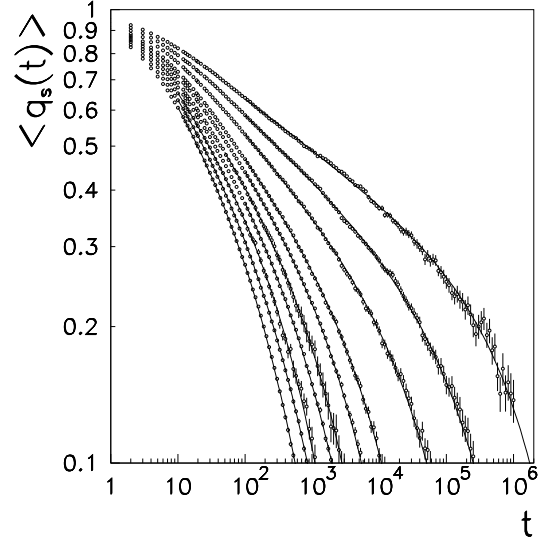


FIG. 7. Relaxation functions of the spin self-overlap, for system size  $20^3$  and chemical potentials  $\mu = 2.583, 2.665, 2.747, 2.829, 2.911, 2.997, 3.083, 3.264, 3.456, 3.661$ . Continuous lines are fits with the function  $ct^{-x} \exp(-(t/\tau)^\beta)$ .

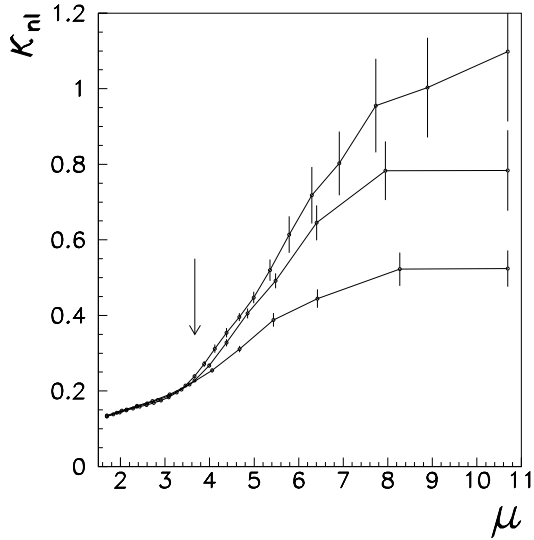


FIG. 6. Non-linear compressibility  $\kappa_{nl}$  as a function of the chemical potential, for sizes  $6^3, 8^3$  and  $10^3$ . The arrow marks the point where spin variables display the transition.

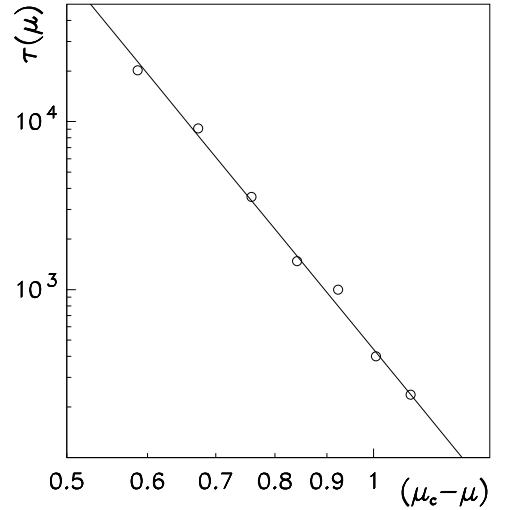


FIG. 8. Relaxation times  $\tau$  of the spin self-overlap, as obtained by the fits of Fig. 7, for chemical potentials  $2.583 \leq \mu \leq 3.083$ . The straight line is a fit with the function  $|\mu - \mu_c|^{-z\nu}$ , and  $\mu_c = 3.67$  fixed, which gives  $z\nu = 7.4$ .

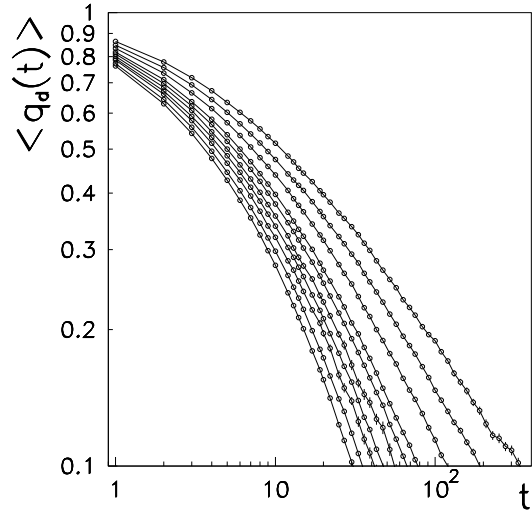


FIG. 9. Relaxation functions of the density self-overlap, for the same system size and chemical potentials of Fig. 7.

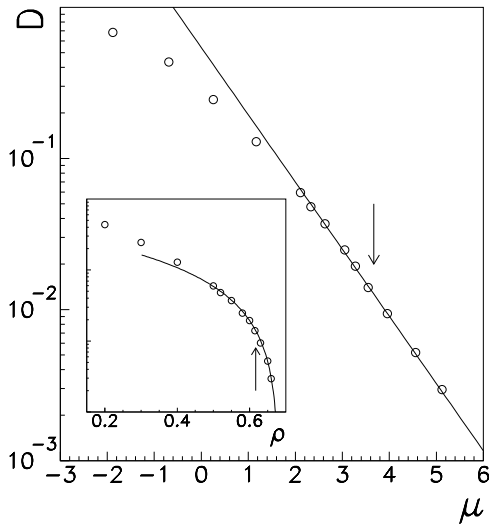


FIG. 10. Diffusivity as a function of the chemical potential, for a system size  $16^3$ . The solid line is a fit with the Arrhenius form  $D = ae^{-\alpha\mu}$ . Inset: Diffusivity as a function of the density. The solid line is a fit with the power law  $D = a(\rho_0 - \rho)^\gamma$ , with  $\rho_0 = 0.681$  and  $\gamma = 1.38$ . The arrows mark the point where the spin variables display the transition.